PAPER • **OPEN ACCESS**

Multimode interference self-imaging optical fiber sensor based on sol-gel silica for methane detection

To cite this article: Muhamad Fairul Izwan bin Mat Zain and Nor Ain Binti Husein 2023 *J. Phys.: Conf. Ser.* **2432** 012014

Journal of Physics: Conference Series **2432** (2023) 012014 doi:10.1088/1742-6596/2432/1/012014

Multimode interference self-imaging optical fiber sensor based on sol-gel silica for methane detection

Muhamad Fairul Izwan bin Mat Zain[a], Nor Ain Binti Husein[a]

[a] Department of Physics, Faculty of Science, Universiti Teknologi Malaysia, 81310 Johor

Abstract. We reported a multimode interference (MMI) sensor based on single mode fiber-no core fiber-single mode fiber (SMF-NCF-SMF) structure incorporated with silica sol-gel nanostructure for detection of methane. Due to the core mismatch between SMF and NCF, a number of higher order modes was excited at the NCF region and recoupled back to the fundamental mode of SMF lead-out which resulted in multimode interference self-imaging. Deposition of silica sol-gel nanostructure formed the hybrid waveguide whose optical property changes according to the surrounding perturbation. The effect of silica coating upon its thickness was clearly demonstrated which can enhance the sensitivity of the sensor. As the concentration of methane varies, the effective refractive index of the waveguide also changes, hence introducing the resonant dip shifts in the transmission spectrum. The sensitivity achieved was 7.92 nm/% for 8-layers of coating, 5.47 nm/% 4-layers of coating, and 0.5 nm/% for uncoated sensor. In addition, the proposed sensor also exhibits good linear response within 0 - 0.175 % of methane concentration while the test of reproducibility confirmed the sensing stability of the sensor.

1. Introduction

Over the last two centuries, methane concentrations in the atmosphere have more than doubled, largely due to human-related activities. Methane is one of the greenhouse gasses which its excessive presence can contribute to atmospheric global warming potential [1]. Due to its nature that is short-lived as compared to carbon dioxide, achieving significant reduction in its production could potentially contribute to significant effect on the atmosphere. One of the potential solutions to reduce the methane leakage to atmosphere is by having a detection system that can detect the methane present at particularly low concentration as a precautionary measure. Nevertheless, it remains challenging to trace the emission of methane which exhibit colourless and odourless characteristics. Currently, method such as Fourier Transform Infra-Red (FTIR) spectroscopy [2] and gas chromatography [3] has widely been used which can measure the concentration down to ppb level, but these methods are costly, slow response, and not in situ. Meanwhile, optical fiber sensor (OFS) is another type of optical sensor that has gained a lot of interest due to its outstanding characteristics such as simple, inexpensive and in-situ detection.

It is important to mention that the performance of OFS is governed by its sensing structure, detection technique and functionalized coating. To date many optical fiber structure modifications have been introduced, including cladding removal [4], tapering [5] , bending[6], and mode mismatch [7]. The

purpose of the modification is to allow the evanescent field to be accessible to the surrounding. Consequently, various detection schemes can be configured such as Evanescent wave absorption [8], interferometer [9], Bragg grating [10] and plasmonic resonance [11]. In addition, functionalized materials such as graphene [11], metal-organic framework [4], fluoro-siloxane (UVCFS) nano-film encapsulated cryptophane A [12] and tin oxide [7] can be incorporated along the waveguides in order to improve the overall sensitivity and selectivity of the sensor. Recently, the performance of cladding removal of plastic optical fiber decorated with PDMS and ZIF-8 MOF was tested to measure methane concentration up to 50 %. The sensor, which was primarily designed for methane leakage detection, was proven selective against nitrogen, pure oxygen and water vapour due to the adsorption property of PDMS and ZIF-8 that favour methane molecules [4]. A simultaneous measurement between methane and hydrogen was performed using photonic crystal fiber utilizing SPR as detection scheme [12]. The formation of distinct peaks which correspond to both gases distinctly was utilized through matrix demodulation to achieve the sensitivity of −1.99 nm/% and −0.19 nm/% for hydrogen and methane respectively. Another scheme that utilized hybrid composition of graphene-CNT-Nanotubes-Poly (MethylMethacrylate) as the sensing layer succeeded to achieve the detection within 100 ppm level [11]. In this scheme, silver was used as dielectric material to achieved the plasmonic reaction with the evanescent field produced from the unclad fiber. For the first time, no-core-fiber decorated with nickel was fabricated as reflectance-based for methane detection [9]. Compared to other fiber structures, NCF has some distinct advantages such as high evanescent wave penetration and good structure integrity.

Here, in this paper, we present the core mismatch structure based on SMF-NCF-SMF decorated with silica sol-gel nanostructure for methane detection within less than 1 % concentration level. Due to the mismatch of core diameter between the waveguides at SMF-NCF boundaries, the evanescent field will leak to the cladding part of NCF hence allowing the surrounding perturbation. The presence of silica nanostructure will form the hybrid waveguide whose optical property varies corresponds to the adsorption of methane. By monitoring the wavelength shift attributed to the adsorption of different methane concentrations on the coating, a sensing scheme is established.

2. Sensor Structure and Principle

The working principle of the sensor is based on multimode interference self-image effect as illustrated in Figure 1 [13]. When incident light propagates from the lead in SMF into the NCF structure, the fundamental mode will be excited into a series of higher-order modes within NCF region, which include both core mode and cladding modes [14]. The light will further propagate and recouple into lead out SMF as fundamental mode, which results in multimode interference. The relationship between the interaction length, L and self-image numbers produced, p is,

$$L = p\left(\frac{3L_\pi}{4}\right) \tag{1}$$

Where L_π is the beat length which can be further formulated as,

$$L_\pi = \frac{4\Delta n_{eff} D^2{}_{NCF}}{3\lambda_m} \tag{2}$$

Where λ_m is free space wavelength, D is diameter of NCF and Δn_{eff} is effective refractive index of NCF. Combining equation (1) and equation (2), the free space wavelength is denoted as,

$$\lambda_m = p\left(\frac{\Delta n_{eff} D^2 {}_{NCF}}{L}\right) \tag{3}$$

From Equation (3), it could be deduced that as L decreases while D_{NCF} and Δn_{eff} increase, the free space wavelength, λ_m also increases. In other word, when the external RI increases, the free-space wavelength of the NCF fiber structure will shift into the longer wave. By calculating the wavelength interval, the characterization of methane concentration through changing the refractive index of the external environment RI can be established. In addition, incorporation of sol-gel silica which exhibit porous structures can attribute to better adsorption of analyte molecules. Due to the presence of multiple functional groups such as Si-O-Si and Si-OH, the realization of sol-gel silica is ideal solution to capture the small molecules such as CH_4 by forming the surface hydrogen bonds [15]. As the methane molecules present, the adsorption of methane with the silica nanostructure at the cladding-air interface took place via physisorption which subsequently affect the hole concentration of silica. As a result, the conductivity of the material will decrease which affect the carrier density of the material. Hence, the RI of the material will also be affected according to the equation [16] ,

$$N(\omega) = n(\omega) + ik(\omega) = \sqrt{\varepsilon} = N_1 + iN_2 \tag{4}$$

where, n, k, ε, N_1 and N_2 are an index of refraction, extinction coefficient, permittivity, and carrier density respectively.

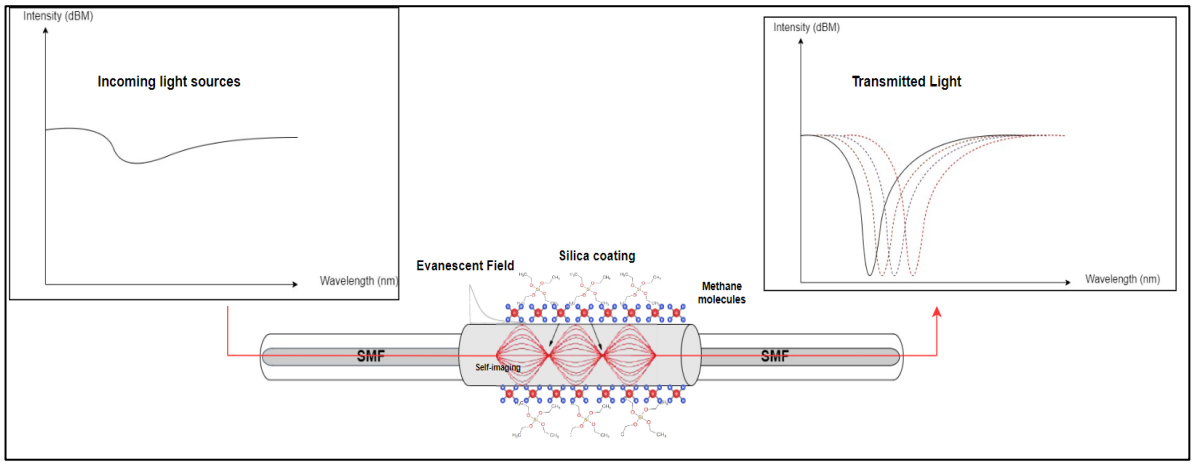

Figure 1. Schematic diagram of multimode interference self-imaging upon light transmission and silica-methane interaction.

3. Experimental Details

The fabrication of the sensor mainly involved three steps which were preparation of sensing head, synthesization of sol-gel silica and the deposition of the nanostructure on the sensing head to form a thin film.

3.1 Sensing Head Fabrication

The sensing head was prepared by cleaving and fusion splicing the different fibers, namely SMF and NCF to from SMF-NCF-SMF structure. The cleaving process was carried out using mechanical cleaver, FC-6S, Sumitomo Electric, Tokyo, Japan. The fusion splicer used is Z1C, Sumitomo Electric, Tokyo, Japan with the arc power and duration time set to default. The fibers employed in this experiment are conventional step-index SMF NCF (Thorlabs, United State) and step-index NCF (Thorlabs, United State) whose core diameters were 9 and 128 μm, respectively. A portion of no-core fiber (NCF) of defined length 90 mm was sandwiched between two SMFs to form a hetero-structured fiber. During the cleaving and splicing, both ends of the fibers were cleaved with minimal cleave angle and aligned precisely to avoid any mechanical offset which could compromise the MMI effect. The end cleaved angles and fiber offset in this experiment was ensured not to exceed 0.3º at both ends and 0.1 μm respectively. The advantage of using NCF is the outer structure requires no further modification such as chemical etching, polishing, or tapering that usually weakens them. Hence, the proposed sensor has the advantage of retaining its robustness.

3.2 Sensor Functionalization

Sol gel silica was synthesized by mixing tetraethyl orthosilicate (TEOS), ethanol, deionized water and hydrochloric acid (HCL) with the ratio 1:2:0.5:0.01 as shown in Figure 2 [17]. The solution was stirred using an electromagnetic stirrer for 1 hours and stored in the fridge at 13 ℃. Next, approximately 50 μL of silica sol-gel nanostructure was dropped onto the entire sensing region and left for 15 minutes before forming another coating layer. To ensure the successful bonding between fiber and the coating, the probes were left at room temperature for 24 hours at room temperature. The absorbance spectra from the Attenuated Total Transmission Fourier Transform Infrared Spectroscopy, ATR-FTIR (Perkin Elmer) confirmed the successful synthetization and deposition of silica sol-gel by the occurrence of Si-O-Si peaks at 1056 cm^{-1} and 798 cm^{-1} while formation of Si-OH bond at 962 cm^{-1} and 1695 cm^{-1} as shown in Figure 3 [18].

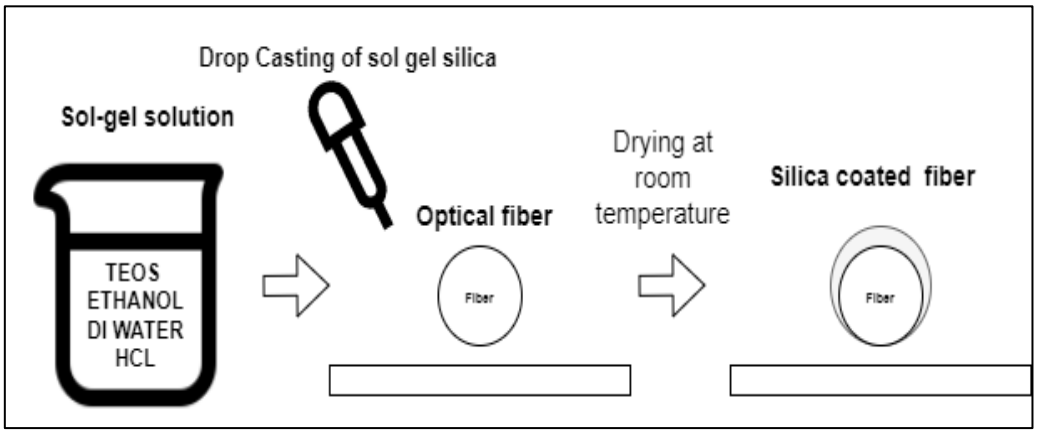

Figure 2. Sol Gel Deposition on the fiber.

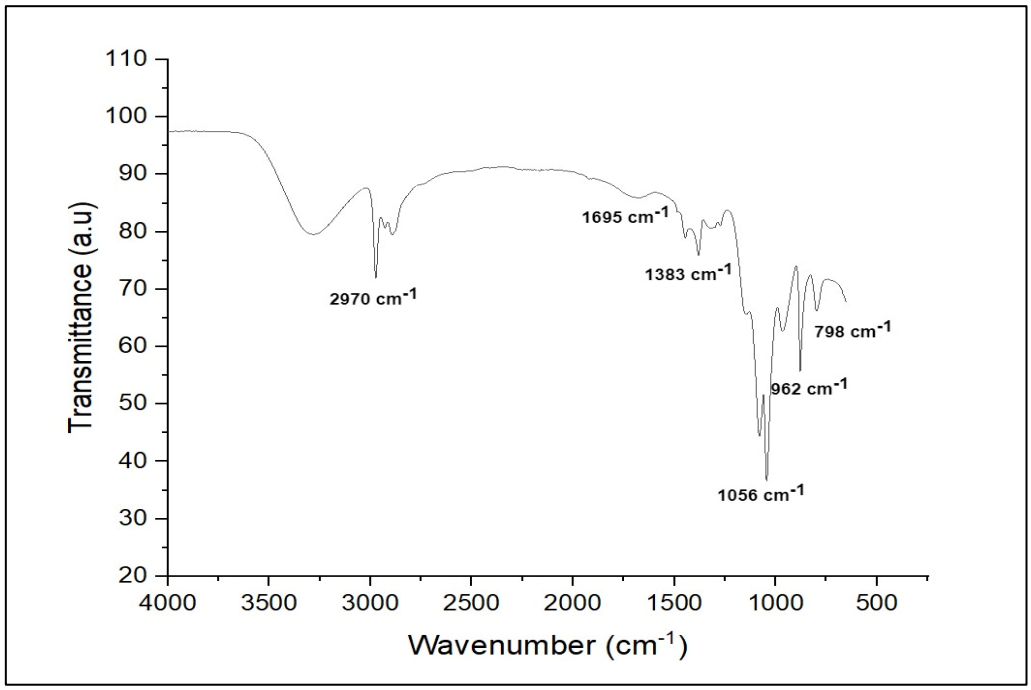

Figure 3. Absorbance spectra from FTIR.

4. Experimental Result and Discussion

The performance of the sensor was demonstrated using the optical setup as shown in Figure 4**.** Amplified Spontaneous Emission -Light source (Fiberer) with wavelength range 1525-1565 nm was used as the incident light source which was connected to the end of the SMF-pigtail of the sensor. The other end of the SMF-pigtail was connected to the Optical Spectrum Analyzer (Yokogawa AQ6370D) with wavelength range 600 to 1800 nm. The OSA resolution was set at 0.2 nm. A specially designed cylindrical chamber with inlet and outlet was used to contain the fiber. In order to ensure the consistency of transmission spectrum obtained in the experiment, each sensor was kept straight and ensured uninterrupted to avoid the fiber bending that can compromise the reliability of the experiment. The surrounding temperature was kept constant at 20°C under normal atmospheric pressure throughout the experiment. Before the measurement, the chamber was purged with nitrogen gas in order to remove any impurities and the reference spectrum was taken after the signal stabilised. After that the mixture of nitrogen gas 99.5 % and methane gas 99.5 % was injected gradually to the chamber. The specific flow rate was set precisely using mass flow controller (MKS). The concentration of methane was calculated using the following equation,

$$concentration\ (\%) = \frac{Mass\ flow\ rate\ (sccm)}{Mass\ flow\ rate\ (sccm)} \times 100 \tag{5}$$

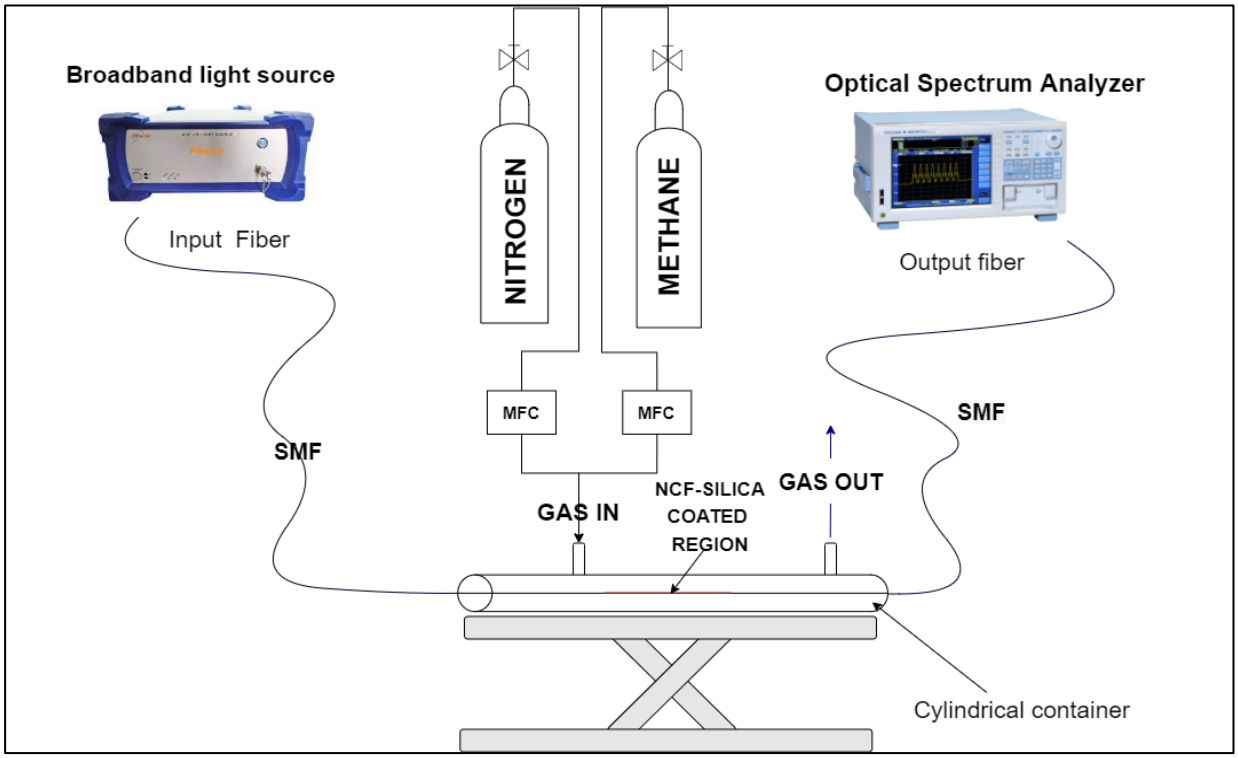

Figure 4. Experimental setup for methane detection.

From the OSA interface, the observation of the dip for uncoated,4-layers and 8-layers of coating sensor was selected at 1538.60, 1541.2, nm, 1543.2 nm respectively. The shifting toward longer wavelength corresponds to the thickness of coating layers which affect the effective refractive index of the sensors. As the methane concentration increased, more methane molecules adsorbed on the surface of the sensor. Hence, the dip will now move toward shorter wavelength due to the change of refractive index of the cladding, which is in agreement with Equation (3), as shown in Figure 5 (a). The slope of the graph represents the sensitivity of the sensor, where the highest sensitivity achieved was 13.89 nm/% in the range 0 to 0.175 % for 8-layers coating and 3.81 nm/% within 0.175 to 0.375 % as illustrated in Figure 5 (b). The similar pattern was observed for 4-layers coating with the sensitivity recorded at 8.35 nm/% and 2.92 nm/% at both ranges respectively. Meanwhile, the uncoated sensor exhibits the lowest sensitivity which was 1.12 nm/% and 0.09 nm/% respectively. The significant different between coated and uncoated sensors demonstrates the role of silica nanostructure as functionalized material to provide enhancement in term of analyte interaction with the waveguide. In addition, the sensor with a thicker sol-gel coating (8-layers) showed better sensitivity which theoretically corresponds to a greater number of functional groups such as Si-O-Si and Si-OH that can capture more methane molecules. The linear responses recorded for all sensors within 0 – 0.175 % are 96.27 %, 98.33% and 98.55 % for the uncoated, 4-layers coating and 8-layers coating respectively. Within higher concentration, the sensor linearity shows significant declining wavelength shift rate which suggests that these sensors might be saturated due to prolonged adsorption of methane. In the meantime, the poor linear response of uncoated sensor may be attributed to poor adsorption property of pristine material (silica dioxide) of sensor. To test the repeatability of the sensor, the sensor of 4-layers coating was injected in with the concentration of 0.1 % of methane and 99 % nitrogen gas consecutively. The wavelength shift occurred at 60 s interval until the signal stabilized at peak level and return to the base value was recorded. From Figure 5 (c), the sensor exhibits minimal variation of maximum (0.1 % methane in) and minimum (nitrogen in) peaks between measurements, which is still in the acceptance range. Furthermore, the dynamic response of the sensor is calculated to be 9 minutes to reach the stable state, while recovery time recorded is 11 minutes. The sensor is concluded to have relatively slow response and recovery time, but the sensor's repeatability is still in the acceptable range. The comparison of our present work with previous works reported was shown in Table 1. It is worth noting that the role of silica nanostructure was clearly manifested as a functionalized layer that can promote more adsorption toward methane.

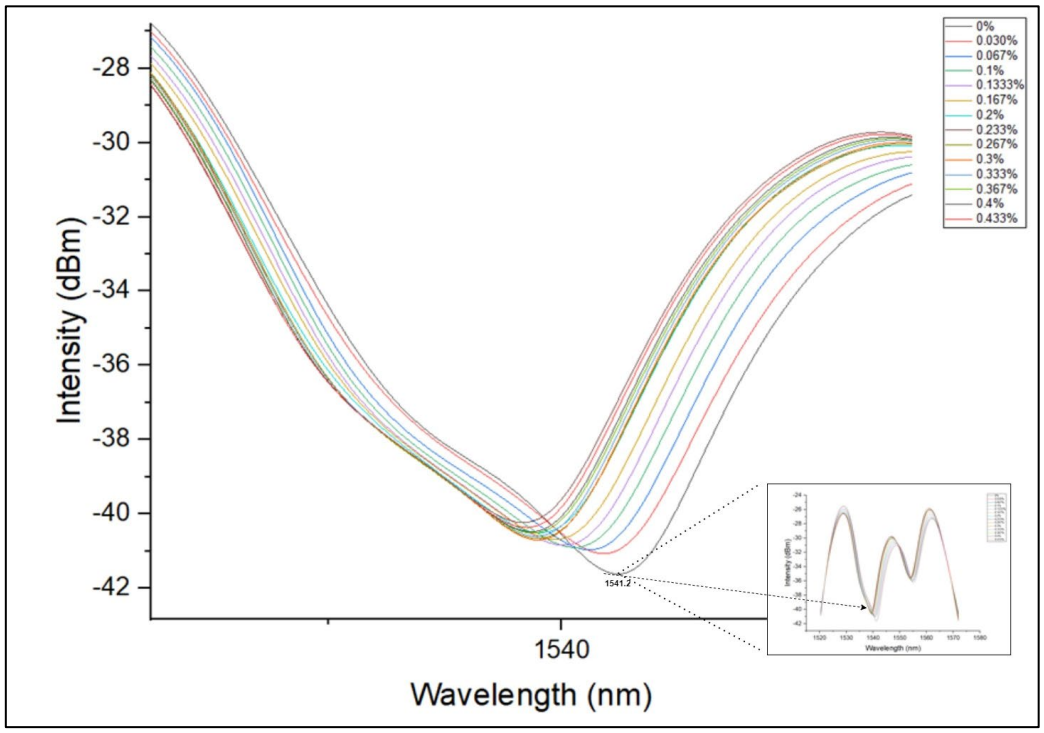
0%
0.030%
0.067%
0.1%
0.1333%
0.167%
0.2%
0.233%
0.267%
0.3%
0.333%
0.367%
0.4%
0.433%
Intensity (dBm)
-28
-30
-32
-34
-36
-38
-40
-42
1540
Wavelength (nm)
1541.2

(a)

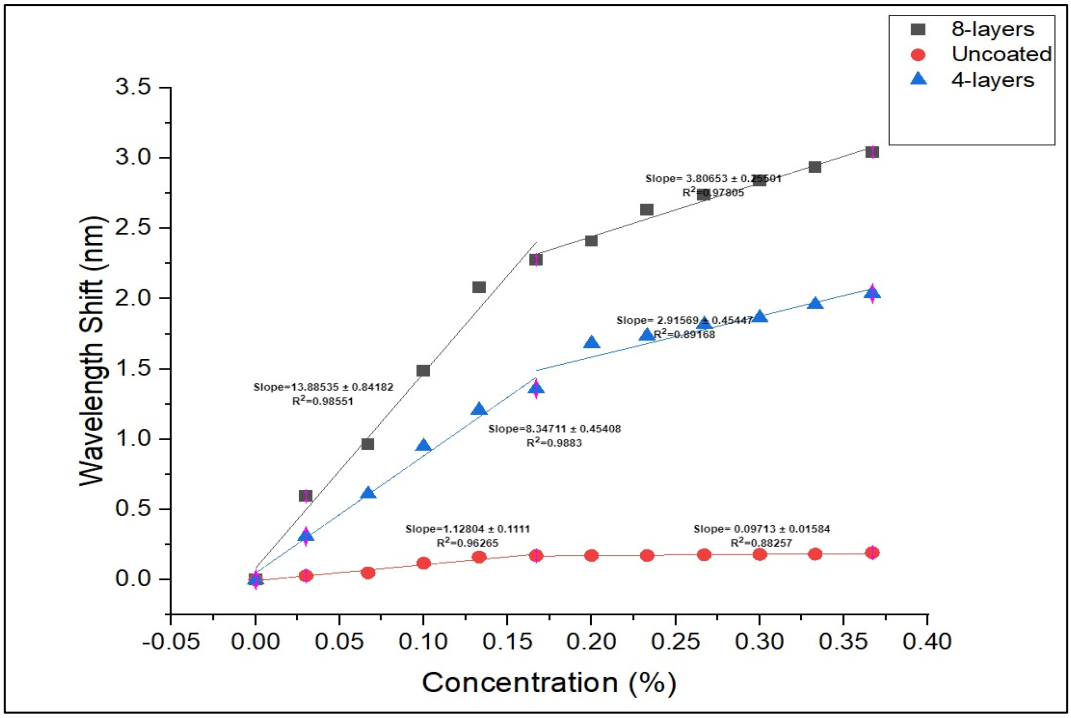
8-layers
Uncoated
4-layers
Wavelength Shift (nm)
3.5
3.0
2.5
2.0
1.5
1.0
0.5
0.0
-0.05
0.00
0.05
0.10
0.15
0.20
0.25
0.30
0.35
0.40
Concentration (%)
Slope= 3.80653 ± 0.25501
R²=0.97805
Slope= 2.91569 ± 0.45447
R²=0.89168
Slope=13.88535 ± 0.84182
R²=0.98551
Slope=8.34711 ± 0.45408
R²=0.9883
Slope=1.12804 ± 0.1111
R²=0.96265
Slope= 0.09713 ± 0.01584
R²=0.88257

(b)

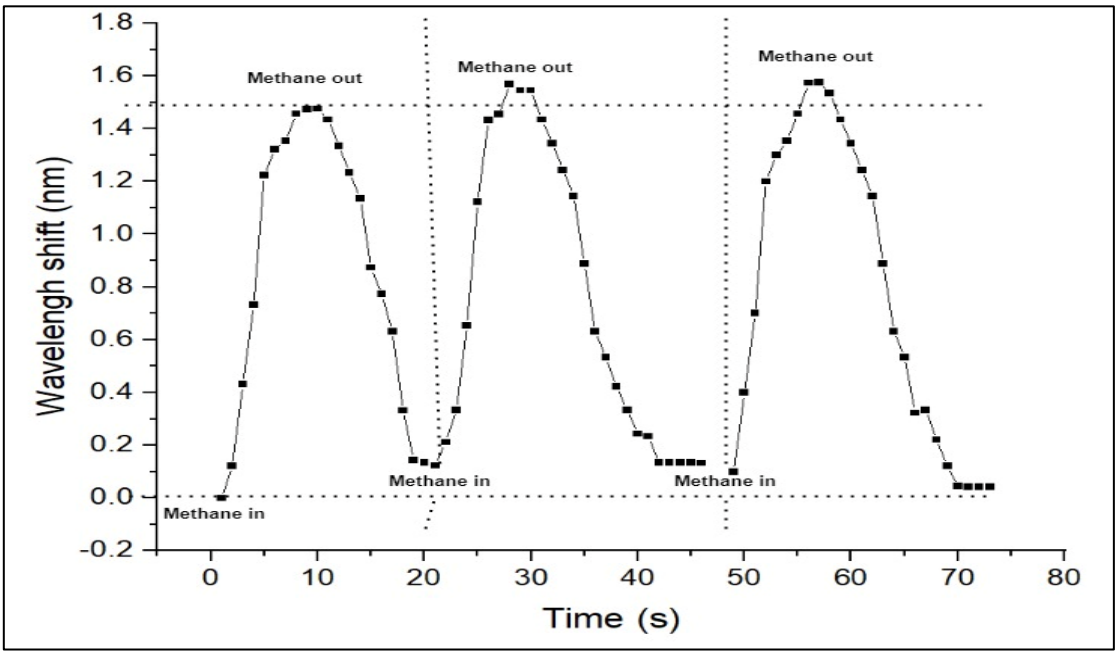

(c)

Figure 5. (a) Transmission spectrum of 4-layers of coating at wavelength 1541.2 as reference wavelength and shifting according to methane concentration. Subset represents the whole transmission spectrum (b) Linear fit of sensing response of sensors with 8-layers, uncoated and 4-layers of coating. (c) Dynamic response at wavelength 1541.2 nm of 4-layers of coating sensor injected with 0.1 % methane and 99% nitrogen gas consecutively for three time repetitively.

Table 1. Comparison of our work with previously reported sensors.

Fiber Structure	Technique	Functionalized Material	Sensitivity	Range	Ref
Etched Fiber	Evanescent Wave Absorption	ZIF-8 MOF	-	1-50 %	[4]
core diameter mismatch	Evanescent Wave Absorption	Cryptophane E	0.0186	0-14.5%	[19]
Reflection-No Core Fiber	Multimode Self-Image	Cryptophanes A/poly-siloxane	0.85 nm/%	0-3.5 %	[9]

Etched Fiber	Surface Plasmonic Resonance	Graphene-Carbon Nanotubes-Poly (Methyl Methacrylate)	-	0-100 ppm	[11]
No-core fiber	Multimode Self-Image	Sol-gel Silica	7.92 nm/%	0-4.3 %	Current Work

5. Conclusion

We proposed the sol-gel coated optical fiber sensor operated based on MMI self-imaging to detect methane at low concentration. The formation of hybrid waveguide between light waveguide and sol-gel nanostructured clearly demonstrated a good adsorption toward methane. Nevertheless, the optimized coating thickness is still in study. The result demonstrated the best sensitivity of the sensor was achieved using thicker sol-gel at 13.885 nm/% with linear response of 98.5 % within 0 – 0.175 %. The utilization of NCF also shows good evanescent field leakage without compromising the structure integrity of the sensor.

6. Acknowledgement

Authors like to acknowledge Universiti Teknologi Malaysia for supporting this research via Research University Grant Tier 2 (Grant Vot. No Q.J130000.2654.16J41)

7. References

[1] Anon Importance of Methane | US EPA
[2] Petersen A K, Warneke T, Frankenberg C, Bergamaschi P, Gerbig C, Notholt J, Buchwitz M, Schneising O and Schrems O 2010 First ground-based FTIR observations of methane in the inner tropics over several years *Atmos Chem Phys* **10**
[3] Loughrin J H, Antle S W and Polk J 2017 A gas chromatographic method for the determination of bicarbonate and dissolved gases *Front Environ Sci* **5**
[4] Cao R, Ding H, Kim K J, Peng Z, Wu J, Culp J T, Ohodnicki P R, Beckman E and Chen K P 2020 Metal-organic framework functionalized polymer coating for fiber optical methane sensors *Sens Actuators B Chem* **324**
[5] Harun S W, Lim K S, Tio C K, Dimyati K and Ahmad H 2013 Theoretical analysis and fabrication of tapered fiber *Optik (Stuttg)* **124**
[6] Tan A J Y, Ng S M, Stoddart P R and Chua H S 2020 Theoretical Model and Design Considerations of U-Shaped Fiber Optic Sensors: A Review *IEEE Sens J* **20**
[7] Zhang J Y, Ding E J, Li Z H, Xu S C, Wang X X, Li X Y and Ma K W 2019 An improved tin oxide core mismatch optical fiber sensor and its preparation method *Optical Fiber Technology* **48**
[8] Zhang J Y, Ding E J, Xu S C, Li Z H, Wang X X and Song F 2017 Sensitization of an optical fiber methane sensor with graphene *Optical Fiber Technology* **37**

[9] Li S, Li X, Yang J, Zhou L, Che X and Binbin L 2016 Novel Reflection-type Optical Fiber Methane Sensor Based on a No-core Fiber Structure *Materials Today: Proceedings* vol 3
[10] Mohammed H A and Yaacob M H 2020 A novel modified fiber Bragg grating (FBG) based ammonia sensor coated with polyaniline/graphite nanofibers nanocomposites *Optical Fiber Technology* **58**
[11] Mishra S K, Tripathi S N, Choudhary V and Gupta B D 2015 Surface Plasmon Resonance-Based Fiber Optic Methane Gas Sensor Utilizing Graphene-Carbon Nanotubes-Poly(Methyl Methacrylate) Hybrid Nanocomposite *Plasmonics* **10**
[12] Liu H, Wang M, Wang Q, Li H, Ding Y and Zhu C 2018 Simultaneous measurement of hydrogen and methane based on PCF-SPR structure with compound film-coated side-holes *Optical Fiber Technology* **45**
[13] Xiao G, Zhang K, Yang Y, Yang H, Guo L, Li J and Yuan L 2020 Graphene oxide sensitized no-core fiber step-index distribution sucrose sensor *Photonics* **7**
[14] Morshed A H 2011 Self-imaging in single mode-multimode-single mode optical fiber sensors *Saudi International Electronics, Communications and Photonics Conference 2011, SIECPC 2011*
[15] Fan X, Deng S, Wei Z, Wang F, Tan C and Meng H 2021 Ammonia gas sensor based on graphene oxide-coated mach-zehnder interferometer with hybrid fiber structure *Sensors* **21**
[16] Narasimman S, Balakrishnan L and Alex Z C 2018 Fiber-optic ammonia sensor based on amine functionalized ZnO nanoflakes *IEEE Sens J* **18** 201–8
[17] Liu D, Han W, Mallik A K, Yuan J, Yu C, Farrell G, Semenova Y and Wu Q 2016 High sensitivity sol-gel silica coated optical fiber sensor for detection of ammonia in water *Opt Express* **24**
[18] Gui-Long X, Changyun D, Yun L, Pi-hui P, Jian H and Zhuoru Y 2011 Preparation and characterization of raspberry-like SiO2 particles by the sol-gel method *Nanomaterials and Nanotechnology* **1**
[19] Yang J, Xu L and Chen W 2010 *Chinese Optics Letters* **8**